Journal of Integrated Coastal Zone Management / Revista de Gestão Costeira Integrada 20(1):61-78 (2020)
http://www.aprh.pt/rgci/pdf/rgci-n281_Ceregeiro.pdf | DOI:10.5894/rgci-n281

Revista de Gestão Costeira Integrada
Journal of Integrated Coastal Zone Management

Tidal Farm Electric Energy Production in the Tagus Estuary

José Maria Ceregeiro[@ 1], Manuel Duarte Pinheiro[2], Francisco Javier Campuzano[3]

[@] *Corresponding author: jmsasceregeiro@gmail.com*
[1] *Instituto Superior Técnico.*
[2] *Instituto Superior Técnico. Email: manuel.pinheiro@tecnico.ulisboa.pt*
[3] *Instituto Superior Técnico. Email: campuzanofj.maretec@tecnico.ulisboa.pt*

ABSTRACT: The exponential population growth and increasing world energy consumption has prompted the World to search for new forms of renewable energy that could curb our dependence on fossil fuels, in order to safeguard the world's environment from the looming threat of climate change. Tidal energy is arguably one of the most promising renewable solutions to replace and diversify part of the energy supply. This is due to the tide's high predictability and technological maturity when compared to other renewable sources, as it is an untapped market with room for development. The main goal of this work is to explore the viability of powering the river-side urban areas, namely Oeiras and Lisbon, through the Tagus' tidal energy. Such is accomplished by modelling the Tagus estuary's hydrodynamics through MOHID – a water modelling software developed by MARETEC, at the Instituto Superior Técnico. Different simulations were made, for different river water discharges throughout the year, so as to determine the behavior of said tidal farm over the course of one year. To simulate the energy production that this solution would generate, two calculation modes were used – one through the use of theoretical equations to predict the energy production of a tidal farm, and the other through the use of MOHID's built-in tool to assess a tidal turbine's energy production. In the end, an economic assessment of such a solution is presented, based on current tidal energy costs.

Keywords: Tidal Energy; Tidal Energy Converter (TEC); Levelized Cost of Energy (LCOE); MOHID; Tidal turbine; Simulation.

RESUMO: O crescimento populacional e o consequente aumento do consumo de energia mundial originou a procura de novas formas de energias renováveis que pudessem reduzir a nossa dependência em combustíveis fósseis, de forma a salvaguardar o Ambiente da ameaça iminente das alterações climáticas. A energia das marés é uma das possíveis soluções para substituir e diversificar parte do fornecimento de energia. Isto deve-se à elevada previsibilidade das marés e da maturidade das soluções tecnológicas existentes quando comparadas com outras fontes de energia renovável, dado que se trata de um mercado inexplorado com espaço para desenvolvimento. O objetivo principal deste trabalho é explorar a viabilidade de alimentação das zonas urbanas ribeirinhas, nomeadamente Oeiras e Lisboa, através da energia das marés do estuário do Tejo, através da modelação do estuário do rio Tejo com o

* *Submission: 25 AGO 2019; Peer review: 8 SEP 2019; Revised: 16 MAR 2020; Accepted: 16 MAR 2020; Available on-line:25 MAY 2020*

MOHID, um software de modelação hidrodinâmica desenvolvido pelo MARETEC, no Instituto Superior Técnico. Diferentes simulações foram feitas, para diferentes descargas do rio, para determinar o comportamento de um hipotético parque de turbinas ao longo de um ano. Foram usados dois modos de cálculo para estimar a energia que esta solução produziria – um através do uso de equações teóricas para prever a produção de energia de um campo de aproveitamento de energia das marés, e outro através do uso de uma ferramenta incorporada no MOHID para determinar a produção de energia de uma turbina. No fim, é apresentada uma avaliação económica dessa solução com base nos custos atuais de energia das correntes de marés.

Palavras-chave: Energia das marés; Conversor da Energia das Marés (TEC); Custo Nivelado de Energia (LCOE); MOHID; Turbina de marés; Simulação.

1. INTRODUCTION

The growing human population is putting an increasingly bigger strain on the world's resources, specifically on the amount of fossil fuel that is burned to power our ever-increasing energy needs. This is hailed as being one of the world's most important problems: to generate enough clean energy to guarantee human consumption without harming the environment (Castro-Santos *et al.*, 2015).

The looming threat of climate change has prompted policy makers such as the European Union to adopt targets to limit carbon dioxide emissions and utilize energy from renewable sources in order to curb the environmental impact of our energy needs. However, traditional renewable energy sources such as solar and wind power may not always be available, as they are highly influenced by weather patterns. It is therefore necessary to expand the sources of renewable energies, so as to diversify their origin and thus rely less on fossil fuels to power our energy needs.

By having most of its population within 50 km of the sea, Portugal has a great potential to power urban areas through ocean energy. Tidal power is a largely untapped energy source that is, for the most part, uninfluenced by weather patterns.

Tidal energy can be harvested through tidal stream energy or tidal barriers. This work will mainly focus on the potential of tidal stream energy to power coastal urban areas near the Tagus estuary, since the country's low tidal range of roughly 3 m (Antunes, 2013) renders the application of tidal barrier solutions purposeless (U.S. Energy Information Administration (EIA), n.d.).

Although it is in its infancy, tidal energy has the potential to be a significant renewable energy contributor, as studies indicate that the global theoretical resource is approximately 3 TW, of which 1 TW is harvestable in coastal areas (Kempener and Neumann, 2014).

By having a channel that acts like a choking point, the Tagus estuary has a large potential for the application of tidal current energy solutions, as the water is forced to undergo a converging effect much like the Venturi effect as it goes in-and-out of the estuary due to tidal action, thus generating powerful currents that are capable of electric energy production.

2. TIDAL ENERGY

Tidal energy is a form of hydropower that converts the energy from the natural rise and fall of the tides into electricity. This phenomenon is caused by the combined effects of the gravitational forces exerted by the Moon, the Sun and the rotation of the Earth. This cyclical vertical movement of the sea levels is also accompanied by variable horizontal movements, designated by tidal currents (Owen, 2008).

This pulling effect from both the Moon and the Sun, however, can work in accordance or in opposition to one another, thus resulting in spring tides and neap tides, respectively. The tide's range is at its maximum when all three celestial bodies line up with each other, culminating in higher high tides and lower low tides. Neap tides on the other hand happen when the celestial bodies' gravitational pull alienates each other, causing less extreme tidal variation (Hammons, 2011).

In general, tides are influenced by the Moon's behavior, where the tidal amplitude is influenced by the lunar cycle (29.5 days), while the tidal frequency is influenced by the lunar day (24h50min) and geographical characteristics. Depending on the location of the planet, there can be three main types of tides when it comes to their daily frequency: semidiurnal, mixed and diurnal tides. The tides experienced on the Portuguese coastline (as is for most of the world) are of semidiurnal nature. Semidiurnal tides are characterized by having a tide period of 12h25min, meaning that there are two high-tides and two low-tides every lunar day, as is shown in Figure 1. Tides can also be diurnal, meaning there's only one high-tide and one low-tide per lunar day, or mixed, where high-tides and low-tides have different heights between each other (O Rourke *et al.*, 2010).

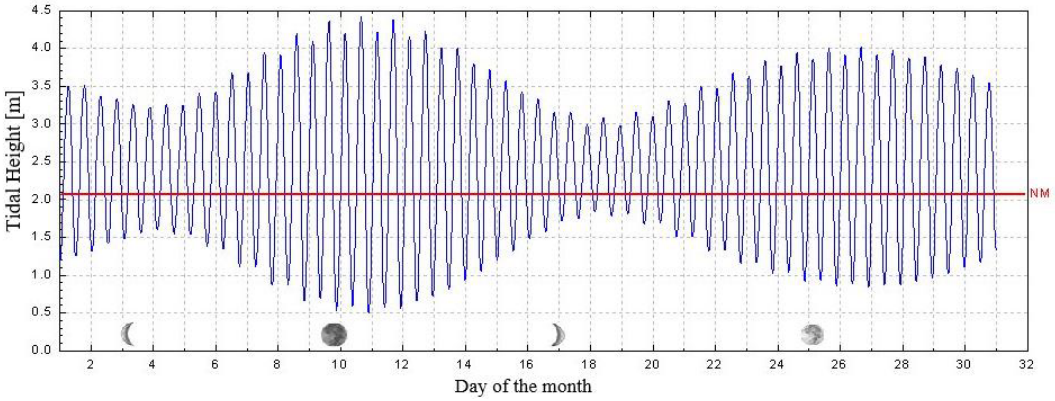

Figure 1. Tidal profile in Lisbon, September 2018 (FCUL, n.d.).

2.1 Technologies

Tidal energy consists of potential and kinetic components, thanks to the elevation in the water level and the resulting currents, respectively. Hence, tidal power technologies can be categorized into two main types: tidal range and tidal current technologies, which take advantage of a tide's potential and kinetic energy, respectively (O Rourke *et al.*, 2010).

2.1.1 Tidal range

Tidal technologies take advantage of the potential energy created by the difference in water levels through the use of tidal barrages. The principles of energy production of a tidal barrage are similar to a dam, except that a tidal barrage is built across a bay or estuary and that tidal currents flow in both directions (O Rourke *et al.*, 2010).

Tidal barrages work primarily by closing its valves once the tide reaches its maximum height, so as to trap the water inside the basin, or estuary. As the tide recedes and it reaches its minimum height, the valves are opened, letting the water flow through hydropower turbines, which keep generating electricity for as long as the hydrostatic head is higher than the minimum level at which the turbines can operate efficiently (Kempener and Neumann, 2014; Prandle, 1984).

However, given that the conventional tidal difference between high-tide and low-tide for the use of tidal barrages is 5-10 m, this renders the application of this solution in Portugal purposeless, as the average tidal difference in Portugal is roughly 3 m (Antunes, 2013). For this reason, this work focuses only on the tidal current potential of the Tagus estuary.

2.1.2 Tidal current

Unlike tidal range technologies, tidal current or tidal stream technologies make use of the tide's kinetic energy, converting it into electricity, in a manner similar to how wind turbines work (O Rourke *et al.*, 2010). The available tidal power [W] of a tidal current is given by the following equation:

$$P = \frac{1}{2} ApU^3 \quad (1)$$

where U is the velocity of the water flow [m/s] through the specific area A [m^2], and ρ is the water density [kg/m^3].

Considering that water is 832 times denser than air, a tidal rotor can be smaller and turn more slowly than a wind turbine, while still delivering a significant amount of power (O Rourke *et al.*, 2010).

Unlike photovoltaic panels or wind turbines, tidal turbines are hardly influenced by weather conditions, which grants them a high predictability. However, there is not one device technology design that trumps above the others as the overall consensual design of what a tidal turbine should look like. As such, TEC devices fall into four main categories.

Horizontal-axis turbines work similarly to wind energy converters, in the way that they exploit the lift that the fluid flow exerts on the blade, forcing the rotation of the turbine that is mounted on a horizontal axis (parallel to the direction of the water flow), which in turn is connected to a generator, converting mechanical energy into electrical energy (World Energy Council, 2016).

Despite resembling wind turbine generators, marine rotor designs must also consider factors such as reversing flows, cavitation and a harsher environment like salt-water corrosion, debris and having to endure greater forces due to the water's higher density (Lewis *et al.*, 2011).

The working principle of Vertical Axis Turbines is similar to the one described above, except that the turbines are mounted on a vertical axis (perpendicular to the direction of the water flow).

Enclosed tips turbines are essentially horizontal-axis turbines that are encased in a Venturi tube type duct. This is made in order to accelerate and concentrate the fluid flow that goes through the turbines, taking advantage of the Venturi effect (World Energy Council, 2016).

Oscillating hydrofoils consist of a blade called a hydrofoil (shaped like an airplane wing) located at the end of a swing arm, which moves up-and-down. This pitching motion is used to pump hydraulic fluid through a motor, which in turn is converted to electricity through a generator (World Energy Council, 2016).

2.2 Tidal Energy Challenges

The deployment of TEC devices can have a wide array of benefits. However, they do not come without drawbacks, and being a relatively new technology means that they have a lot of uncertainties related to them. As such, tidal energy devices need to overcome several challenges in order to become commercially competitive in the global energy market.

The barriers to the development of these technologies can be categorized in: (1) technical barriers, that are inherent to the characteristics of the environment in which the devices are inserted, as the fact that being in water makes them more difficult to maintain, or the fact that salt water has a corrosive effect on materials; (2) environmental issues that can arise from the deployment of TEC devices, such as posing a navigation hazard for vessels; (3) financial, economic and market barriers – since tidal energy is a fairly new technology when compared to more mature technologies such as wind and solar power, funding is proving to be one of the most difficult challenges to overcome, since investors are not interested in high-risk demonstration projects that lack sufficient grid infrastructure, whose primary benefits lie in learning and experience rather than financial returns; (4) political and social barriers, such as public acceptability from coastal communities that tend to be suspicious of new sea-related activities, as they could pose conflicts of interests (Kempener and Neumann, 2014).

Given how horizontal-axis tidal turbines receive 76% of all R&D funding (Corsatea and Magagna, 2014), this work focuses only on the hypothetical deployment of a tidal farm solution composed of said turbines.

Given the wide range of existing energy conversion technologies, it is necessary to develop a standard by which the various technologies can be compared to one another, in order to properly assess the cost of a specific technology. One such standard is the levelized cost of energy, or LCOE.

The LCOE of a given technology is the ratio of total lifetime expenditure over the total lifetime output, or electricity generation, reflecting the average cost of capital. This means that an electricity price above this value yields a greater return on capital, while a price below it would yield a loss on capital (Corsatea and Magagna, 2014; U.S. Energy Information Administration, 2018). The LCOE is therefore given by Eq. (2).

$$LCOE = \frac{Life\ time\ cost\ (€)}{Life\ time\ energy\ production\ (kWh)} \qquad (2)$$

A project's lifetime cost can be grouped into two main generic categories: *Capex* (capital expenditures), that include the initial upfront expenses, and *Opex* (operational expenditures), which are the operation and maintenance costs (O&M) (IEA, 2016). It can be stated that CAPEX costs represent 60% of a tidal farm deployment expenditure, while OPEX costs represent the other 40%, both of which can be broken down by cost category, as is shown in Table 1:

Table 1. Tidal LCOE breakdown by cost category (IEA, 2016; Ocean Energy Systems, 2015).

CAPEX (60%)	%	OPEX (40%)	%
Project development	4	Material costs	7
Grid connection	7	Transport costs	32
Device	29	Labour costs	2
Mooring and Foundation	10	Production losses costs	2
Installation	9	Fixed expenses	57

An early assessment of tidal energy's LCOE (Kempener and Neumann, 2014) placed at-the-time demonstration projects to be in the range of 0.25-0.47 €/kWh, while estimating that this value should be between 0.17-0.23 €/kWh by 2020. A more recent study in tidal energy LCOE, however, forecasts an LCOE of 0.17 €/kWh for a tidal farm deployment of 100 MW, 0.15 €/kWh if it's 200MW and 0.10 €/kWh if it's 1GW, in 2018 (Smart and Noonan, 2018).

This evidence is corroborated by Segura *et al.* (2017) who place an LCOE for a tidal energy project in a non-commercial stage (meaning higher risks and uncertainties) and for current TEC technology at 0.15 €/kWh, with values between 0.12-0.15 €/kWh being predicted.

As such, an LCOE value of 0.15 €/kWh for a tidal farm deployment is assumed for the remainder of this work, for a considered service life of the tidal farm of 20 years, similarly to that of an offshore wind farm (Det Norske Veritas, 2014).

3. MOHID SOFTWARE

MOHID is an open source, three-dimensional water modelling system, developed continuously since 1985 by MARETEC, mainly at the Instituto Superior Técnico (IST) from the Universidade de Lisboa, Portugal.

It is a modular system based on finite-volumes where each module is responsible for the management of a certain kind of information, which in turn will be communicated to other modules and the system will run under a single executable program. At its core is a fully 3D hydrodynamics model which is coupled to modules that handle, among others, water quality, discharges, oil dispersion, atmosphere processes. An important feature is MOHID's ability to run nested models, which enables the study of local areas, by obtaining the boundary conditions from the "father" model. Every model can have one or more nested "child" models, and the number of nested models that a simulation can have is only limited by the amount of the available computing power (MARETEC, n.d.).

The versatility of the modular structure allows for the model to be used in virtually any free surface flow water mass. The MOHID Water model has been applied to many coastal and estuarine areas worldwide and has shown its ability to simulate successfully very different spatial scales from large coastal areas to coastal structures (Campuzano *et al.*, 2017).

The Tagus river Mouth operational model runs the MOHID numerical model in full 3D baroclinic mode with a variable horizontal grid cell resolution of 120x145, ranging from 2 km on the ocean boundary to 300 m around the estuary mouth. The model's vertical discretization consists of a mixed vertical geometry, composed of a 50-layer domain. The first 7 layers from the water surface until 8.68 m deep are of a sigma domain, which are on top of a cartesian domain of 43 layers, with their thickness increasing towards the bottom (Campuzano *et al.*, 2017).

The model's horizontal domain is defined by its bathymetry, where a value is attributed to each one of the grid cells mentioned above. This is arguably the most essential information needed to run any MOHID Water simulation.

As for the remaining boundary conditions, the Tagus river Mouth model has an open boundary on the ocean side, receiving hydrodynamic and ecological forcing from the 3D model PCOMS (Portuguese Coast Operational Model System). On the landward side, the Tagus estuary is forced by the river flow, namely the water discharge of the Tagus, Sorraia and Trancão rivers (Campuzano *et al.*, 2017). Figure 2 highlights the aforementioned domains.

In the atmospheric interface, the model is forced by atmospheric results obtained from a 3 km resolution WRF model application performed by the IST Meteorological team (Campuzano *et al.*, 2017).

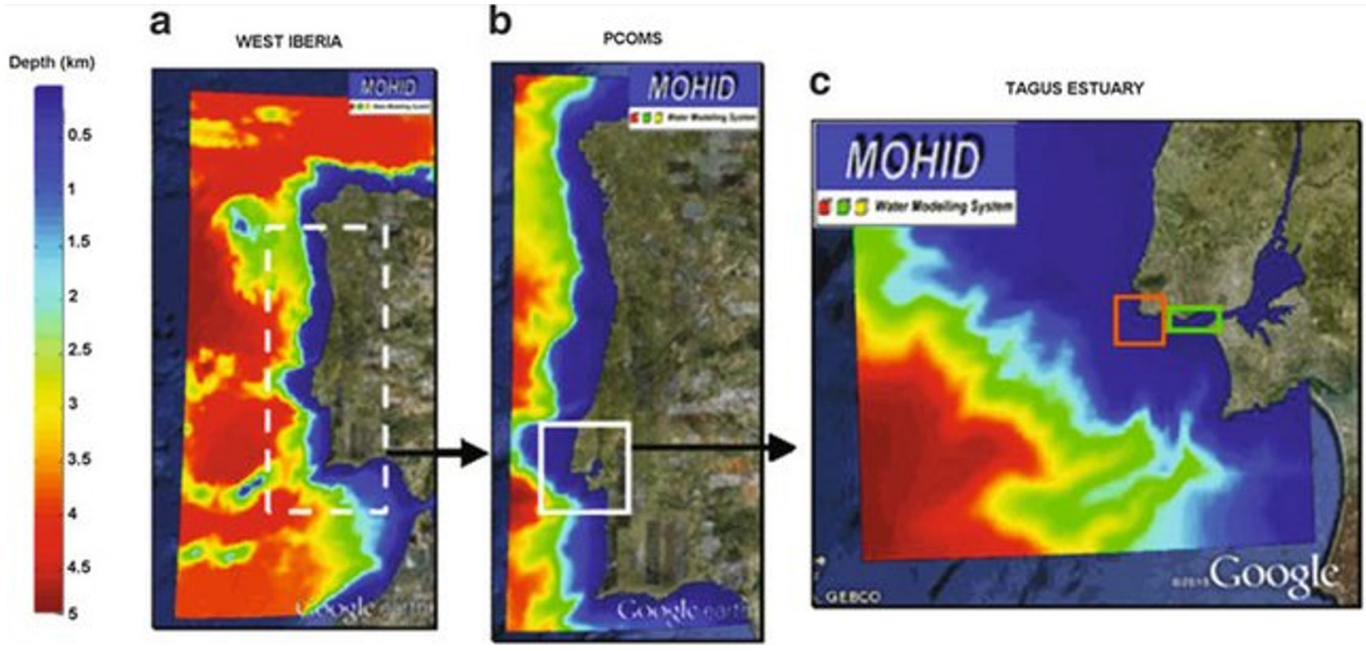

Figure 2. Nested domains used to implement the Tagus model. The domain on the left (a) provides tidal boundary conditions to the PCOMS model (b), which supplies hydrodynamic and bio-geochemical boundary conditions to the Tagus model (c) (Campuzano *et al.*, 2017).

4. CASE STUDY: TAGUS ESTUARY

The Tagus is the longest river in the Iberian Peninsula. Its 1.100 km drain the peninsula's third largest watershed into the Atlantic Ocean, through the Tagus estuary, which is the transition zone between the two (ARH Tejo, 2011).

Morphologically, the Tagus estuary can be divided into four main sections (Portela, 1996), all of which can be visualized in Figure 3. The *fluvial section* is correspondent to the river section that is still influenced by tides, going 30 km inland, with an average width of 600 m; The *upper section* part of the estuary is composed mainly of mudflats, salt marshes and shallow channels that cover 1/3 of the estuary's total area; The *middle section* (or "Mar de Palha") has an average water depth of 5 m; Lastly, the *lower section* is correspondent to a straight and narrow seawater inlet channel about 15 km long and 2 km wide, reaching maximum depths around 45 m. Its narrow nature allows tidal water to undergo a convergence effect similar to the Venturi effect, creating water velocities that make it possible for energy to be extracted, thus making it this work' case study area.

There are two main sources of water inputs into the estuary: fresh water from the rivers and salt water from the tides. The main source of fresh water comes from the Tagus river, which has a mean annual water flow rate of roughly 350 m^3/s, varying seasonally throughout the year with rates typically between 100 and 650 m^3/s (Macedo, 2006). As for other fresh water contributors, Portela (1996) estimates that the Sorraia river's mean annual flow rate is equivalent to around 8.5% of the Tagus' discharge, whereas the remaining effluents have a near negligible flow rate. Figure 4 illustrates the Tagus river average monthly flow rate.

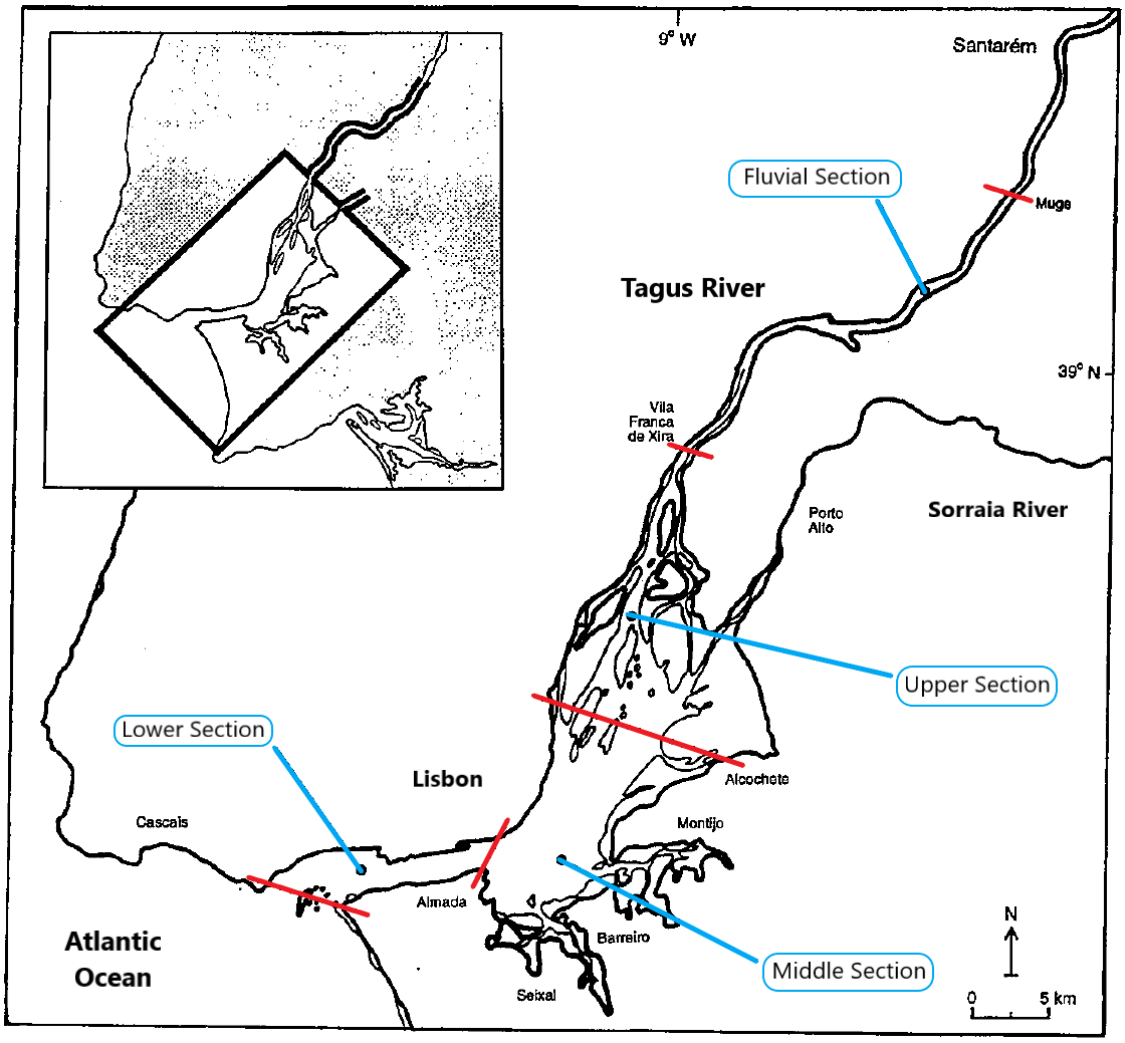

Figure 3. Tagus Estuary (Portela, 1996).

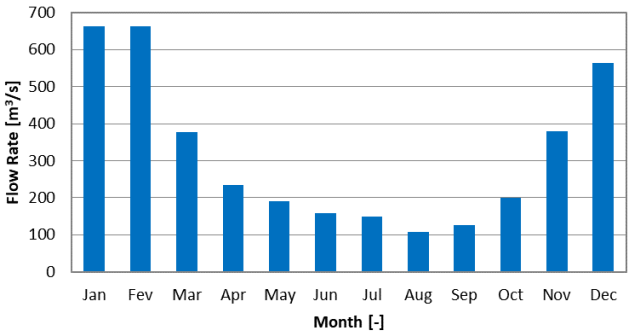

Figure 4. Tagus river average monthly flow rate (1973-2010) (SNIRH, n.d.)

However, the main factor that determines the characteristics of the estuary's hydrodynamic regime is the salt water from the tides. The reason for this is because the average tidal water volume is immense when compared to the estuary's water volume at low tide.

Table 2. Average values for the different tidal reference levels in Lisbon (2010-2018) (Instituto Hidrográfico, n.d.).

	Tide	Level (CD) [m]
HAT	Highest Astronomical Tide	4.28
MHWS	Mean High Water Springs	3.86
MHW	Mean High Water	3.43
MHWN	Mean High Water Neap	3.00
MSL	Mean Sea Level	2.20
MLWN	Mean Low Water Neap	1.42
MLW	Mean Low Water	0.98
MLWS	Mean Low Water Springs	0.54
LAT	Lowest Astronomical Tide	0.17

The estuary's water volume at low tide is 1 900 x 10^6 m^3 (ICNF, n.d.). Given that the mean tidal range is roughly 2.45 m, as is shown in Table 2, this means that an additional 600 x 10^6 m^3 of water is added to the estuary during an average high tide (ICNF, n.d.). This makes up to roughly 26 850 m^3/s between tides, which is the reason behind the powerful tidal currents that are generated.

While the monthly variation of tidal amplitudes are fairly constant throughout the year, the same cannot be said about river discharges, with there being much more water flow during the Winter months than the Summer months.

As such, in order to have a general idea of the amount of energy a tidal farm can generate throughout the year, this work contemplates 3 different simulation scenarios:

- Energy production during a Summer month;
- Energy production during an average month;
- Energy production during a Winter month.

Furthermore, the tidal farm energy resource will be assessed in one of two different ways: according to data processing in the Excel, and through the use of a MOHID Module, named TURBINE Module. This comparison will be made so as to determine whether the TURBINE Module that was coded into the MOHID software is a good enough approximation to the industry's guidelines on how to assess tidal turbines energy potential, or not.

4.1 Modelling the MOHID solution

4.1.1 River discharges

The information regarding the Tagus water flow throughout the year can be accessed in the *Sistema Nacional de Informação de Recursos Hídricos* (SNIRH). It shows that the river has a great seasonal variability, which is why three different scenarios of monthly water discharges were adopted, in an effort to simplify the number of simulations to model: the first simulation will consider a continuous water flux of 110 m^3/s, while the second and third simulations contemplate a continuous monthly discharge of 350 m^3/s and 660 m^3/s, respectively. These values are comparable with the river's average Summer month, average month and average Winter month water discharges.

In Figure 5, both the river's average monthly discharge (in blue) and assumed monthly water discharge for simulation purposes (orange) are displayed.

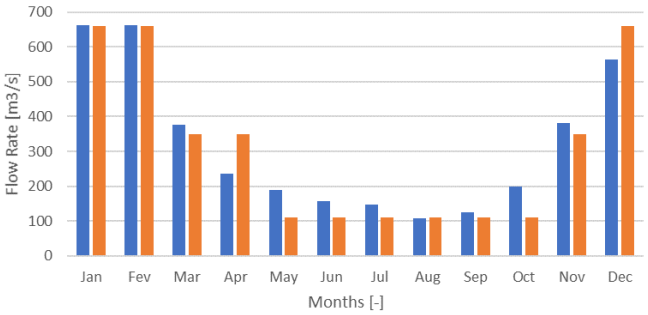

Figure 5. Average Tagus monthly flow rate, 1973-2010.

As for the other freshwater contributors, the Sorraia river's flow rate is adjusted accordingly for each simulation, while other water inputs are considered to be negligible.

4.1.2 Tidal influence

The tidal range found in the area has been obtained from data collected by the tidal gauge located in Cascais. This was done in order to have an overview of the

tidal behavior so that it can be modelled as a boundary condition in the MOHID simulation model. As such, one year-long time series was used to investigate the seasonal variability (displayed in Figure 6), as well as the spring-neap tidal cycles in the area.

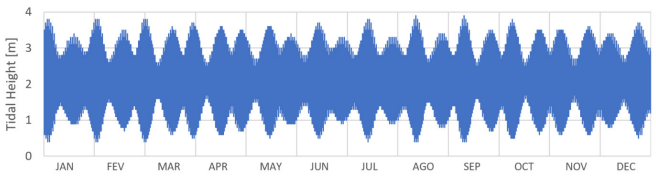

Figure 6 - Tidal height in Cascais during 2018 (Instituto Hidrográfico, n.d.)

Given how the tidal heights caused by the spring/neap cycles remain fairly consistent throughout the year, only the month that is representative of the average tidal range will be considered when modeling the MOHID solution. Table 3 shows each month's average tidal range value.

Table 3 - Tidal range monthly mean values at Cascais.

Month	Mean value (m)	Month	Mean value (m)
January	2.1683	July	2.0817
February	2.1019	August	2.1200
March	2.2217	September	2.1466
April	2.1569	October	2.1196
May	2.1000	November	2.1155
June	2.0621	December	2.0900
Average		**2.1237**	

Monthly tidal range averages show that the month that is representative on the average annual tidal range is August, meaning it will be the one to be used to estimate the average power density during the year. The tidal level profile for the month of August is shown in Figure 7.

The maximum water level variability takes place between the 11th and the 13th, so it is expected for the maximum tidal velocities (and thus the maximum power output) to be reached around those days. Part of this work's analysis will contemplate the differences in a tidal farm's power output throughout the course of one day, for all the different days in one month so as to allow for the prediction of electricity generation in any given moment.

4.1.3 Tidal turbines

Given that no single tidal current technology is currently the 'standard' technology, Legrand (2009) states that a turbine with generic characteristics ought to be used in order to assess the available resources.

When considering the TECs' characteristics, they should follow the following rules (Legrand, 2009):

- A maximum diameter of 20-25m, as that is currently the technological limit of a horizontal axis turbine;
- A minimum top clearance of 5m below the lowest astronomical tide, so as to allow for recreational activities and minimize turbulence and wave loading effects on the TECs, as well as damage from floating materials;
- A minimum bottom clearance of either 5m, or 25% of the water depth (whichever is the greater), to minimize turbulence and shear loading from the bottom boundary layer;
- As for device spacing, the lateral spacing between devices ought to be 2.5 times the rotor diameter (2.5d), whereas downstream spacing should be 10d. The devices should also be positioned in an alternating downstream arrangement.

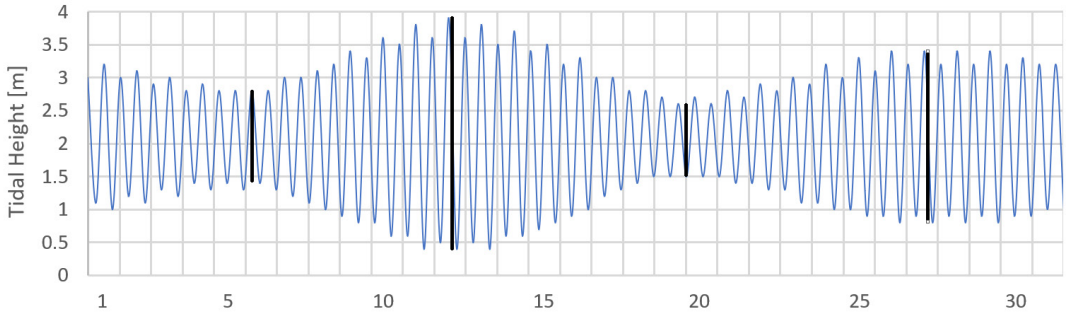

Figure 7. Tidal height in Cascais, during August 2018.

The available kinetic energy of a tidal current was given in Equation (1). However, not all the current's power is susceptible of being transferred to the TEC and transformed in electric energy, as one has to take into account the efficiency of all the mechanisms implicated in that transfer. As such, the power generated by a TEC can be defined as the following:

$$P = \frac{1}{2} A \rho C_P \eta_{PT} U^3 \qquad (3)$$

Where η_{PT} is the powertrain efficiency (generator power/rotor power) and C_p is the rotor power coefficient.

The rotor power coefficient represents the ratio of actual electric power produced by a turbine divided by the total water current power flowing through the turbine at any given current speed. The theoretical maximum rotor power coefficient is given by the Betz's Law. It states that no turbine can convert more than 16/27 (0.593) of the kinetic energy of the current into mechanical energy by turning a rotor (Manwell *et al.*, 2009).

According to Legrand (2009), the rotor power coefficient can be considered to rise linearly from 0.38 at cut-in velocity to 0.45 at the rated velocity. While the former is the minimum velocity required for device operation (necessary to produce the torque needed to rotate the rotor), the latter is the current velocity at which the power output reaches the limit that the electrical generator is capable of.

As for the turbine's powertrain efficiency, it is the efficiency at which a turbine converts mechanical energy into electrical energy, and it is determined by the rotor efficiency, the generator efficiency and the electrical grid efficiency. All in all, the average powertrain efficiency can be considered to be 90% (Legrand, 2009).

4.2 Data analysis

The first thing to consider when determining the best suited areas for implementing a tidal farm is assessing where the greatest energy potential is. In order to do so, the modelled simulation of the estuary with all the parameters mentioned beforehand was run for the three different scenarios of water flow, displayed in Figures 8 to 10.

In order to assess the locations with the highest energy potential, the fifty areas (model cells) with the highest energy density were highlighted, as shown in Figure 11.

The highlighted points remain largely unchanged for the other two simulations (Summer and Winter river discharges). Thus, there is a general trend between the three simulations that the locations with the highest energy potential are located within the regions of Oeiras, Belém and Cais do Sodré.

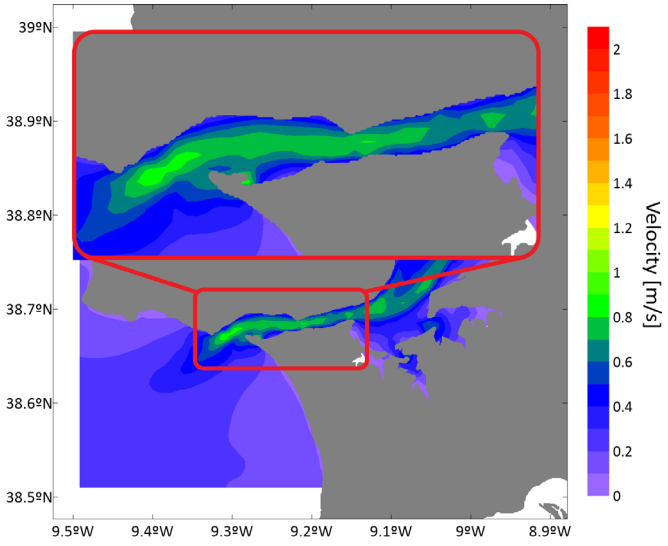

Figure 8. Average water velocity for Summer flow rate simulation.

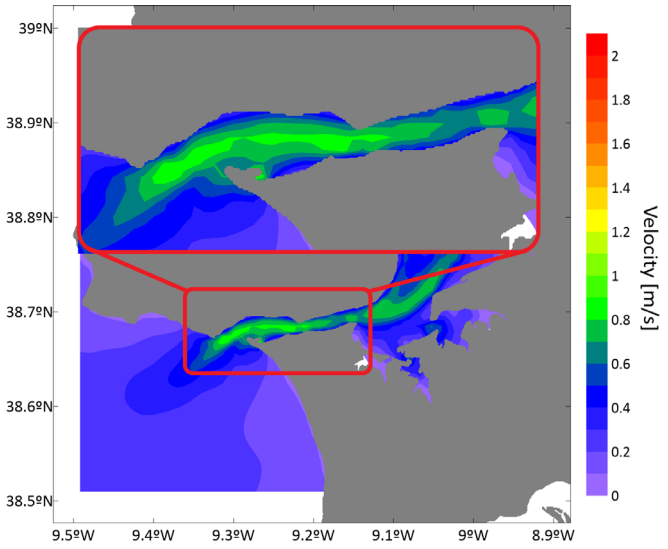

Figure 9. Average water velocity for average flow rate simulation.

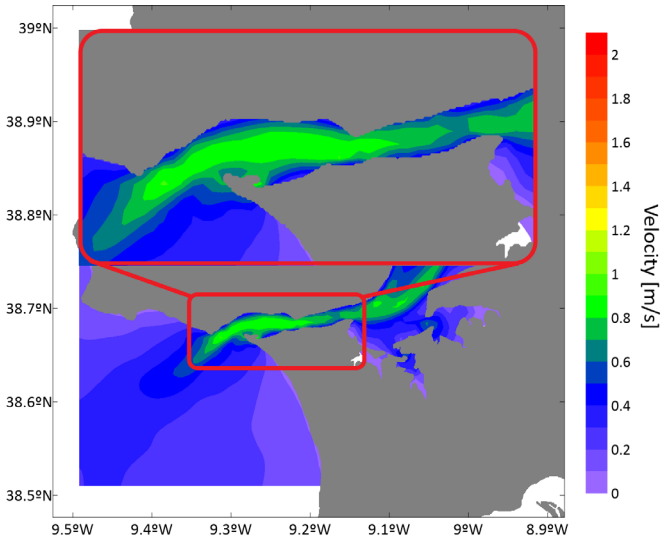

Figure 10. Average water velocity for Winter flow rate simulation.

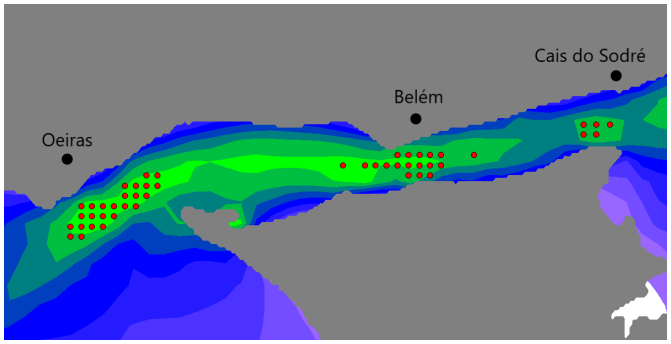

Figure 11. Fifty areas (model cells) with the highest energy density during the average monthly flow rate simulation.

It is worth mentioning that the water channel that connects the Atlantic Ocean to the Tagus estuary is a vital waterway with a large economic importance to the city of Lisbon, as it allows the access of vessels such as cruise ships and cargo ships, which dock in Lisbon's Port. As such, a mandatory approach channel that is 250 m wide (to allow for two-way vessel traffic) has been set, as shown in Figure 12.

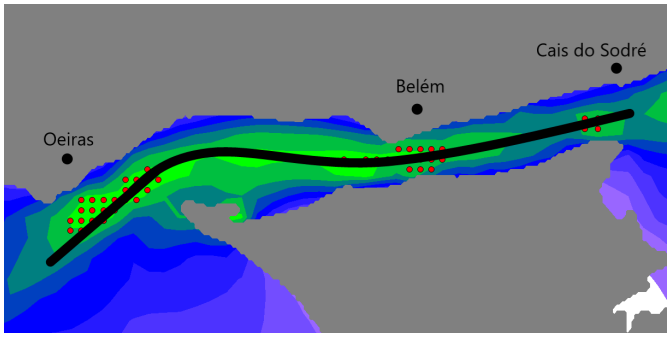

Figure 12. Port of Lisbon's approach navigation channel.

Given the turbines' necessary top clearance of 5 m, other minor vessels such as traffic passenger ships, water-taxis, yachts and recreational ships don't pose a threat to a potential tidal farm, as their draught is usually well below 5 m. Therefore, two energy-production assessments will be made:

- Assuming there are no limits within the estuary channel where a tidal farm could be placed;
- An exclusion zone made of the port's approach channel is taken into account, where a tidal farm cannot be built due to the movement of ships, which rules out several potential sites for implementing a tidal farm.

The comparison between these two assessments is done in order to compare the maximum theoretical energy that a turbine placed in the channel would produce, with the energy produced by a turbine placed in an area that does not interfere with the port's activity. In both assessments, the area used to calculate the energy produced by a turbine is the one with the highest energy potential available in each of the three regions. The selected areas are presented in Figure 13, where the points highlighted in red represent the areas with the maximum theoretical energy potential, and the ones in blue represent the areas with maximum energy potential when taking into account an exclusion zone brought by the port's approach channel.

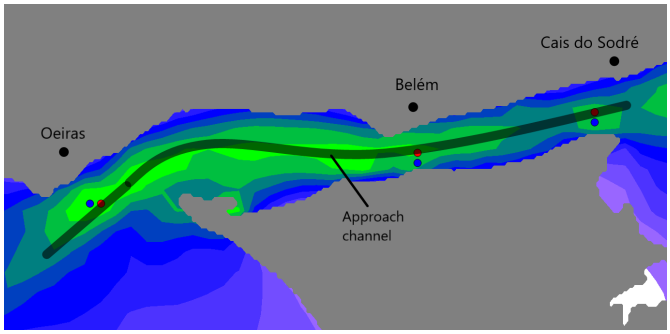

Figure 13. Assessment areas.

4.2.1. Placement of the turbines

Thanks to the boundary shear stress caused by the bottom friction of an open channel, the water velocities will differ over the water depth of each specific area. Considering that tidal turbines are submerged devices, this makes it necessary to determine the vertical distribution of the water velocity on the highlighted areas of interest.

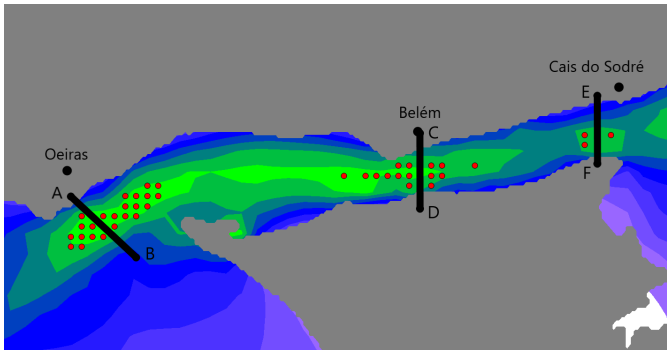

Figure 14. Cross-sections of the regions of interest.

Consequently, three cross sections of the channel were made, in order to visualize the spatial distribution of the average power density per square meter in the regions of interest, for the average flow rate simulation, as shown in Figure 14. This was achieved by inputting the water velocity field values in Equation (1). The results are shown in Figures 15, 16 and 17.

It is easily discernable that there is an area roughly 8-12 m below the sea-level with a high power density, in all three regions of interest. As such, this is seen as the optimal depth at which to place the turbine axis, in order for the turbine to harness the largest amount of energy possible.

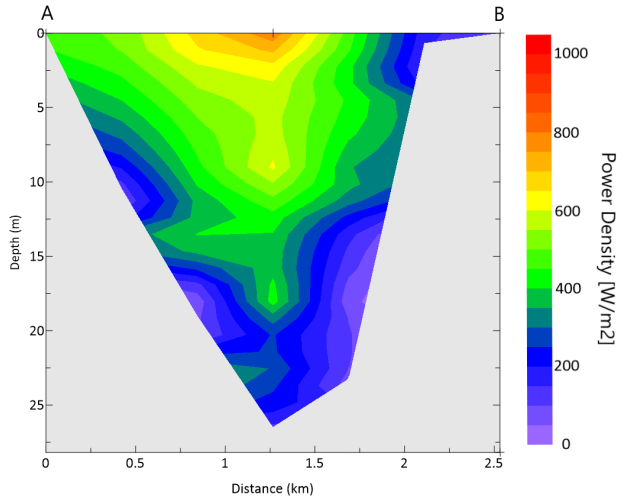

Figure 15. Variation of power density per square meter in Oeiras region.

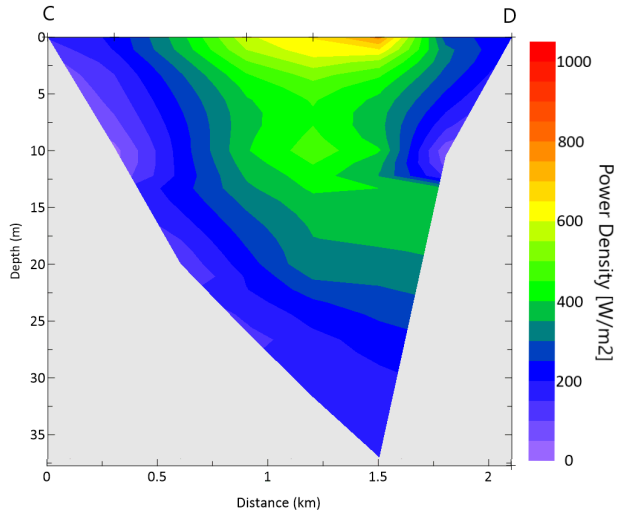

Figure 16. Variation of power density per square meter in Belém region.

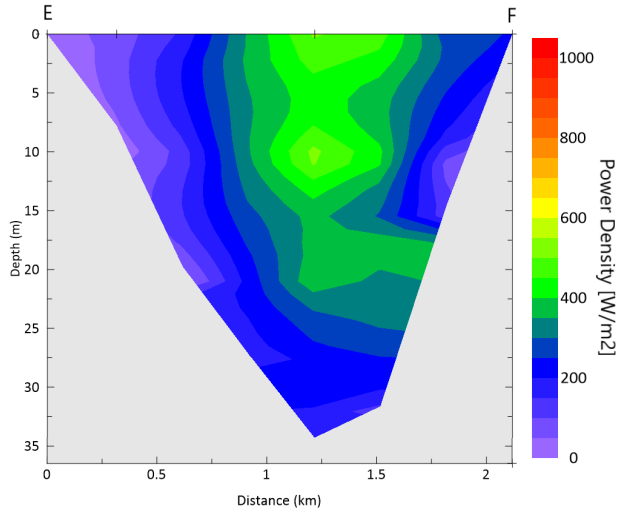

Figure 17. Variation of power density per square meter in Cais do Sodré.

4.2.2. Assessment of the rotors' dimensions

It has already been established, in subchapter 4.1.3, that the diameter of current tidal turbines is limited to 20-25 m, and that they require a 5-meter top clearance and a bottom clearance of 25% of the water depth (or of 5 m, depending on which value is larger).

Table 4 defines the maximum theoretical diameter that a turbine could have in each of the different areas of interest, based on the limitations mentioned above.

Table 4. Maximum theoretical rotor diameter [m] for each area.

	Without Channel	**With Channel**
Oeiras [m]	**14.87**	**11.87**
Water depth [m]	26.50	22.50
Bottom clearance [m]	6.63	5.63
Belém [m]	**18.77**	**22.75**
Water depth [m]	31.70	37.00
Bottom clearance [m]	7.93	9.25
Cais do Sodré [m]	**20.72**	**18.70**
Water depth [m]	34.30	31.60
Bottom clearance [m]	8.58	7.90

Although the different locations have different sized turbines, this isn't necessarily a desirable solution, because rotors could start reaching into velocity fields that aren't necessarily relevant, energy density wise. Another argument against having a different-sized turbines solution is the fact that economies of scale would be lost, adding to the complexity and cost of implementation of such a solution, not only in terms of acquisition of the devices, but also in terms of their maintenance.

As such, this work considers a 15-meter wide tidal turbine for most assessments, except for the Oeiras zone assessment with an exclusion zone. For this case in particular, a 10-meter wide tidal turbine will be considered, due to water depth limitations.

4.2.3. Assessment of velocity fields encompassed by the turbines

Considering the dimensions of the turbines, it is easy to see that the rotors will be subject to various different current velocities, from various different layers in the modelling simulation.

It was previously mentioned in subchapter 3.1 that the model's vertical discretization consists of a mixed vertical geometry, composed of a 50-layer domain. The first 7 layers from the water surface until 8.68 m deep are of a sigma domain, which are on top of a cartesian domain of 43 layers, with their thickness increasing towards the bottom.

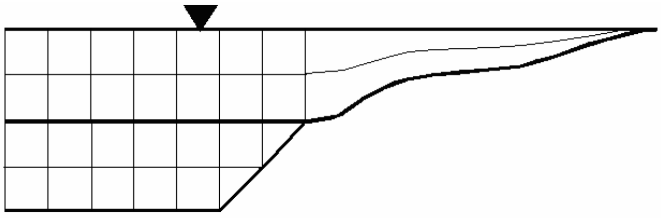

Figure 18. Example of the subdivision of the water column in a Sigma domain (upper 2 layers) and a Cartesian domain (bottom 2 layers).

Given the turbine placement's upper and lower restrictions, their horizontal axis is to be placed at a depth of 12.5 m and 10 m, for the 15 m and 10 m diameter turbines, respectively. This is done so in order to allow for a top clearance of 5 m and in order for the turbines to encompass the layers with the highest velocity fields, as determined in 4.2.1.

Knowing the depth at which to place the turbines and the rotor's diameter, one can assess a turbine's swept area in each model layer by using the following equation,

$$A_{Tk} = \frac{r^2}{2}\,\theta - r\,.\,\sin\frac{\theta}{2}\,.\,d - \sum_{k=1}^{k} A_{Tk-1} \qquad (4)$$

where A_{Tk} represents the turbine's swept area in layer k. As such, the values for U in equation (3) are calculated as:

$$U_{AV} = \frac{\sum_k A_{Tk}\,.\,U_k}{\sum_k A_{Tk}} \qquad (5)$$

where U_{AV} is the average modulus velocity [m/s] of the k layers in the cell of (i,j) coordinates that contains the turbine.

In order to determine the mean annual electrical power produced by a tidal turbine, a histogram analysis for the tidal current speed going through a turbine was carried out. The analysis has been performed by using an interval of 1 hour and a bin size of 0.1 m/s, so as to obtain the percentage of time at which the velocity falls within each bin. The results are shown in Figures 20, 21 and 22.

5. ANALYSIS AND DISCUSSION OF RESULTS

5.1. Annual Energy Production (AEP)

Once the velocity distribution in the area of interest has been estimated, it can be applied to a TEC's power curve, in order to calculate its annual energy output. Since no specific TEC device has been chosen, a generic device will be used for this purpose.

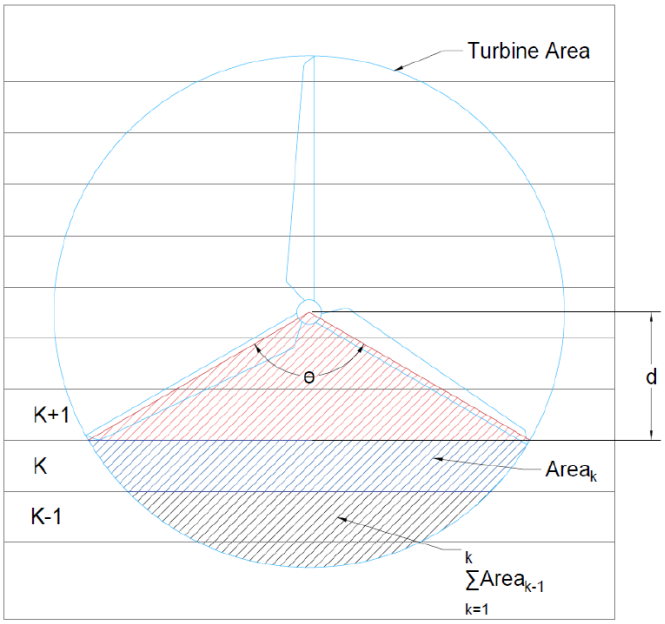

Figure 19. Vertical discretization of the turbine area (Balsells Badia, 2017).

It's already been established that a turbine's rotor power coefficient rises linearly from 0.38 at cut-in-velocity to 0.45 at rated velocity. According to Legrand (2009), a turbine's cut-in-velocity can be considered 0.5 m/s, while its rated velocity (current velocity at which the power output reaches the limit that the electrical generator is capable of) can be taken as 71% of the Mean Spring Peak Velocity (V_{msp}), which is the peak tidal velocity observed at a mean spring tide. Table 5 illustrates each assessment area's rated velocity.

Table 5. Regions' rated velocities (RV) in both assessments.

	Oeiras		Belém		Cais do Sodré	
	without channel	with channel	without channel	with channel	without channel	with channel
[m/s]	2.2	2.2	1.9	2.0	2.0	1.8
RV [m/s]	1.56	1.56	1.35	1.42	1.42	1.28

All the parameters necessary to assess the electrical power generated by a tidal turbine over the course of one year have now been determined. Table 6 presents the calculation of the electrical power and of the mean annual electrical power (AEP) for each velocity bin used in the velocity distributions computation for the Oeiras region without considering an approach channel. The rotor diameter considered here is of 15 m, meaning the turbine has a swept area of 177 m^2.

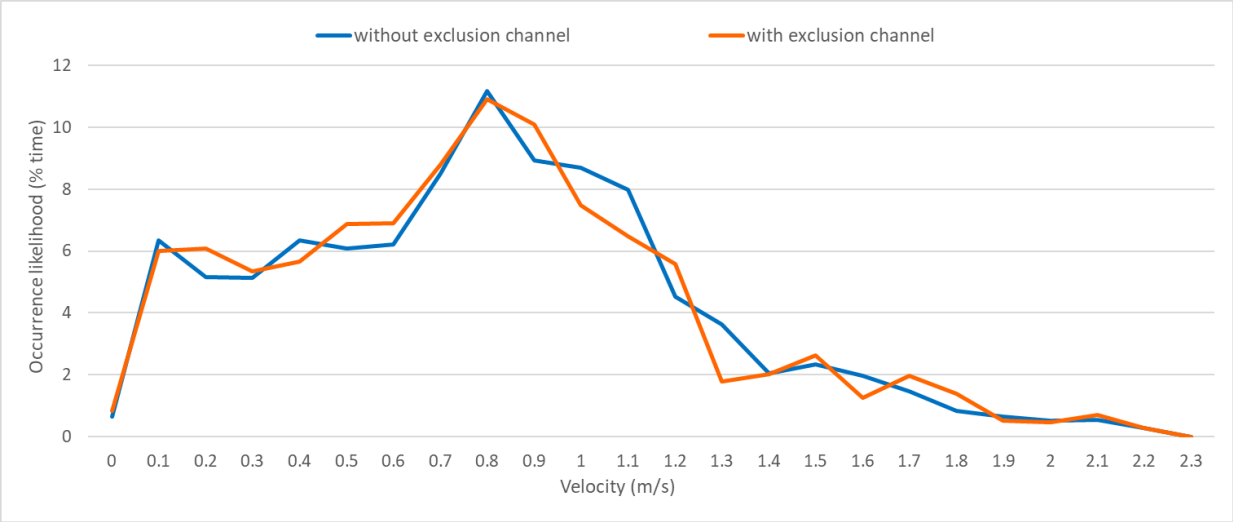

Figure 20. Water velocity distribution in Oeiras turbines.

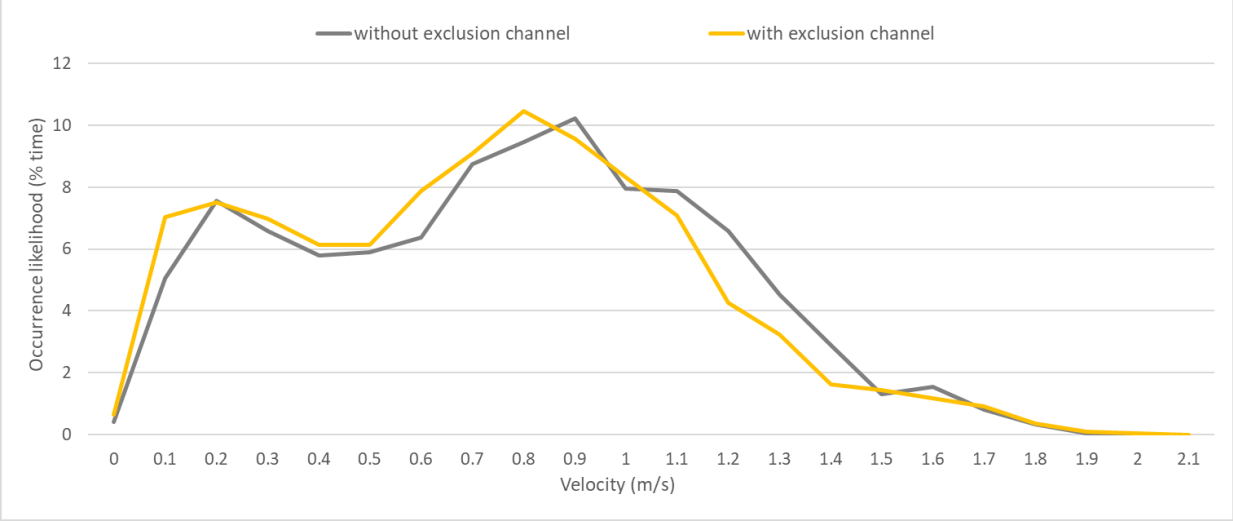

Figure 21. Water velocity distribution in Belém turbines.

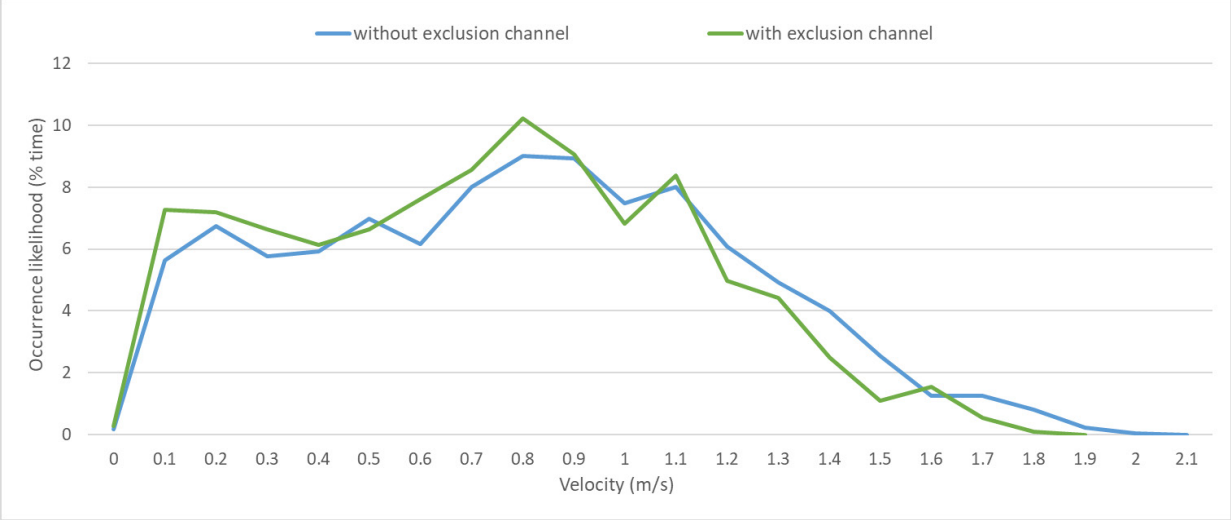

Figure 22. Water velocity distribution in Cais-Sodré turbines.

Table 6. Mean AEP [kW] for Oeiras, without approach channel.

Velocity bin	Occurrence likelihood	Available power	Rotor power coefficient	Electrical power per bin	Mean AEP/bin
[m/s]	[%]	[kW]	[-]	[kW]	[kW]
0	0.64	0.00	0	0.00	0.00
0.1	6.34	0.09	0	0.00	0.00
0.2	5.17	0.72	0	0.00	0.00
0.3	5.13	2.45	0	0.00	0.00
0.4	6.34	5.80	0	0.00	0.00
0.5	6.07	11.32	38	4.30	0.26
0.6	6.21	19.56	39	7.56	0.47
0.7	8.52	31.06	39	12.21	1.04
0.8	11.17	46.37	40	18.54	2.07
0.9	8.93	66.02	41	26.83	2.39
1.0	8.69	90.57	41	37.40	3.25
1.1	7.99	120.54	42	50.57	4.04
1.2	4.53	156.50	43	66.69	3.02
1.3	3.62	198.97	43	86.10	3.12
1.4	2.05	248.51	44	109.18	2.23
1.5	2.35	305.66	45	136.30	3.20
1.6	1.98	370.96	45	155.32	3.08
1.7	1.48	444.95	X	155.32	2.29
1.8	0.84	528.18	X	155.32	1.30
1.9	0.64	621.19	X	155.32	0.99
2.0	0.50	724.53	X	155.32	0.78
2.1	0.54	838.73	X	155.32	0.83
2.2	0.27	964.35	X	155.32	0.42
					34.80 kW

As such, a 15m diameter turbine placed in the highest energy density area of the Oeiras region has a mean annual electrical power of 34.80 kW. As for the annual energy production (AEP) of said turbine, it can be obtained by multiplying the P_{mean} computed above by the available hours per year and the powertrain efficiency, as follows:

$$AEP = 8760 \; . \; \eta_{PT} \; . \; P_{mean} \tag{6}$$

Considering a powertrain efficiency of 90% and that a year has 8760 hours, the turbine's AEP is roughly 274.4 MWh.

The same assessment was done for all other areas of interest, and the results for their AEP are presented in Table 7.

5.2. Monthly Energy Production (MEP)

Although knowing a turbine's AEP is important, it is also relevant to know how this electric energy is produced throughout one month. As such, instead of grouping the velocity data into different velocity bins, the water velocity values were used directly in Equation (3).

Table 7. AEP for a single turbine in the different areas.

	Oeiras		Belém		Cais do Sodré	
	without channel	with channel	without channel	with channel	without channel	with channel
Rotor ø [m]	15	10	15	15	15	15
[kW]	34.80	15.06	28.94	25.52	32.83	25.48
AEP [MWh]	274.37	118.69	228.18	201.20	258.83	200.84

Figure 23 shows the variation in the current velocity through the turbine in the area with the highest energy in the Oeiras region, for the different simulated months:

It is easily discernable that the different river discharges have very little impact on the current velocities that occur during the spring tides, as they pale in comparison to the water input from the tidal action. The same cannot be said during neap tides, as river discharges have a greater ponderosity in the water that builds up in the estuary, meaning higher current velocities during the Winter months.

When putting these values through Equation (3), and attending to the resulting rotor power coefficient, one can assess the turbine's power generation at any given instance during the month, resulting in Figure 24.

It can be concluded that the only instances where the turbine reaches its rated velocity is during the spring tides, as there is a limit to how much power a turbine can produce. It is also easily discernable from this figure that the amount of energy produced by a turbine in the Tagus estuary remains largely unchanged over the course of the year, as a Winter month doesn't produce that much more energy than a Summer month. Cumulatively, this amounts to roughly 22.93 MWh during a Summer month, 23.26 MWh during an average month, and 23.97 MWh during a Winter month. By assuming that a year is composed of 6 Summer months, 3 average months and 3 Winter months, one can also estimate the turbine's AEP, with the results shown in Table 8.

The reason why the AEP values are slightly more conservative than the one's determined in 5.1, is that in that assessment, the current velocities were grouped into velocity bins which can give rise to inaccuracies due to rounding.

5.3. AEP comparison with Module Turbine

In order to determine if MOHID's recently coded module, named Module Turbine, is a good approximation to the industry's guidelines way of assessing a tidal turbine's energy production, a 4th simulation was also computed.

The differences reside with the fact that this Module: (1) considers a constant rotor power coefficient, instead of

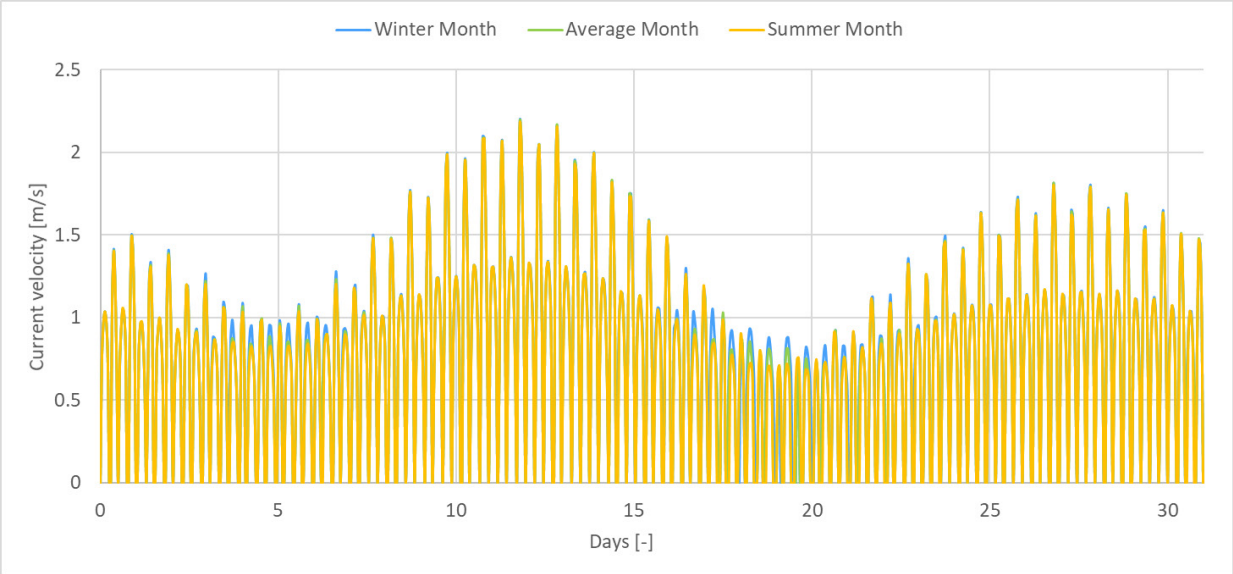

Figure 23. Water velocity through the turbine in the highest energy dense region in Oeiras.

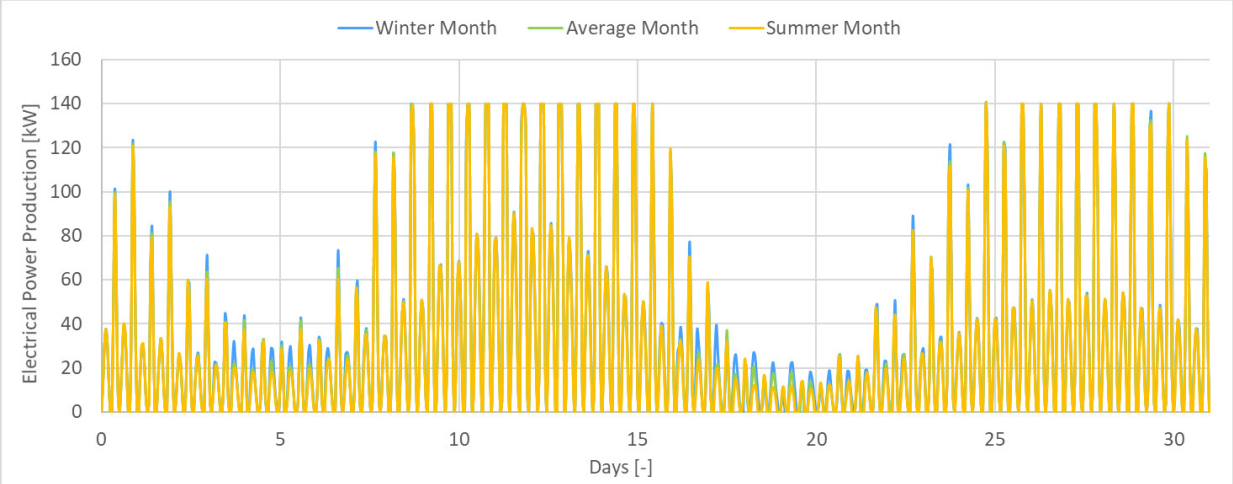

Figure 24. Turbine's energy output throughout the month.

having it rise linearly; (2) it assumes a security factor of 15% of the cut-in-speed (meaning once the rotor is spinning, it will only stop once the current velocity falls below 0.85 times the cut-in-speed); and (3) doesn't take into account the turbine's powertrain efficiency.

This simulation had the exact same specifications as the one for the month with the average river discharge, so as to offer a point of comparison between the two. The difference here is that 6 turbines were placed in the simulation model: one for each of the areas of interest. All of them have the exact same specifications as the ones in the turbines determined above, in terms of location, diameter, cut-in speed, rated velocity and depth at which they are placed.

The sole difference in the turbine's characteristics, is that they were set to have a constant rotor power coefficient of 0.40 from the cut-in speed, to the rated velocity.

Given that only an average water discharge month was simulated this time, the turbine's AEP was calculated considering that one year consists of 12 average water discharge months, instead of the previous assumption of it being composed of 6 Summer months, 3 average months and 3 Winter months. Table 9 compares the results obtained in both methods.

It is clear that the Module Turbine that was coded into MOHID offers, for most situations, a good approximation to a turbine's electrical energy production, even without

taking into account the powertrain efficiency. Where it falls short is when the assessment is made in less energy dense locations. One possible explanation for this is the fact that the turbine's electrical output is stifled by the imposition of a fixed value for the rotor power coefficient, whereas this value varies from 0.38 to 0.45, according to the previous assessment.

Table 8. MEP for one turbine in different assessment areas.

Region	Assessment (Turbine ø)	Simulation	MEP [MWh]	AEP [MWh]
Oeiras	without channel (15m)	Summer	22.93	279.30
		Average	23.26	
		Winter	23.97	
	with channel (10m)	Summer	9.86	120.64
		Average	10.10	
		Winter	10.39	
Belém	without channel (15m)	Summer	18.49	232.54
		Average	19.71	
		Winter	20.82	
	with channel (15m)	Summer	16.41	204.26
		Average	17.30	
		Winter	17.97	
Cais do Sodré	without channel (15m)	Summer	21.18	261.86
		Average	22.19	
		Winter	22.75	
	with channel (15m)	Summer	16.64	203.45
		Average	17.08	
		Winter	17.46	

Table 9. Comparison of the AEP assessed for both methods.

	Oeiras		Belém		Cais do Sodré	
	without channel	with channel	without channel	with channel	without channel	with channel
AEP [MWh]	274.95	111.08	239.18	137.91	255.28	173.88
AEP (5.2)	279.11	121.18	236.50	207.64	266.24	205.00
%	98.51	91.66	101.13	66.42	95.88	84.82

5.4. AEP of a potential tidal farm

When considering the fact that the grid cell size on the simulation model is roughly 300x300m, one can determine how many tidal turbines can be fit in such an area, when looking at the turbines' characteristics, described in 4.1.3. Table 10 shows the number of turbines that can be placed in each area, as well as their cumulative energy production.

Table 10. Tidal farm AEP.

	Oeiras		Belém		Cais do Sodré	
	without channel	with channel	without channel	with channel	without channel	with channel
Turbine ø [m]	15	10	15	15	15	15
Cell size [mxm]	300x300	300x300	300x300	300x300	300x300	300x300
Number of turbines	24	48	24	24	24	24
AEP [GWh]	6.58	5.70	5.48	4.83	6.21	4.82

When considering a tidal farm solution that does not interfere with the Port of Lisbon's activity, one can conclude that a 48-turbine tidal farm solution placed in Oeiras can meet 44% of the county's entire electricity use in order to power the streetlights, as the total consumption sits at 13.11 GWh annually (PORDATA, n.d.-a). As for the city of Lisbon, the other two tidal farms (placed where the Lisbon Port's activities aren't interfered with) can meet 15% of the city's 66.09 GWh electric energy use to power the streetlights (PORDATA, n.d.-a). Alternatively, these solutions would power roughly 2600 and 4300 houses annually, respectively.

5.5 Tidal farm economic analysis

When considering the LCOE value of 0.15 €/kWh determined beforehand, it would cost roughly €16.8 million over the course of 20 years in order to implement the average considered tidal farm in the Tagus estuary (24-turbine tidal farm array with d=15m producing 5.6 GWh/annually). This cost can be further broken into CAPEX and OPEX costs, based on what was said in 2.2.1. which are highlighted in Table 11.

Table 11. LCOE breakdown of average tidal farm in Tagus.

Cost Category	Total Cost
CAPEX [€]	10.080.000
Project development [€]	672.000
Grid connection [€]	1.176.000
Devices [€]	4.872.000 (€203.000/turbine)
Moorings and foundation [€]	1.680.000
Installation [€]	1.512.000
OPEX [€]	6.720.000
Material costs [€/year]	23.520
Transport costs [€/year]	215.040
Labour costs [€/year]	6.720
Production losses costs [€/year]	6.720
Insurance/Fixed expenses [€/year]	191.520

Considering the fact that Portugal's energy supply cost sits at 0.22 €/kWh (PORDATA, n.d.-b), this makes the tidal farm solution in the Tagus estuary (with its LCOE of 0.15 €/kWh) to have an expected breakeven point after 11.25

years, making it a legitimate alternative to power a good part of a nearby county's electricity consumption in order to illuminate the public streets. At the end of the project's life cycle, it would amount to a €7.84 million profit.

6. CONCLUSIONS

It is now more important than ever to diversify our energy sources, since humanity depends too much on fossil fuels to power its needs, and solutions like wind and solar power are dependent on the weather. Tidal power, however, is cyclical and can be predicted to a degree of months in advance.

It has been shown that a small tidal farm composed of only 24 turbines over an area 300x300 m in one of Tagus' river most energy density areas (while considering a vessel approach channel) is able to power on average 2 400 homes for a period of 20 years. Such a project is predicted to cost €16.8 million and it would remove the equivalent of 29 thousand tons of CO_2 emissions from the atmosphere.

Being in close proximity to the power grid and to several ports that can be used to aid in O&M services makes the Tagus estuary an ideal location to implement a tidal farm, as these would imply lesser costs and logistics in order to maintain such an infrastructure. Its close proximity to the power grid also translates into a less extensive underwater power cable, further reducing the tidal farm's CAPEX costs.

It has also been shown that the Module Turbine that was coded into the MOHID software is a good approximation to the industry's guidelines of a tidal turbine's electrical energy output, based on a location's hydrodynamic characteristics, namely the water current speed. This proves that using it in a MOHID simulation model for assessing any area of interest's energy potential will provide with a good estimate of the amount of electrical energy that a tidal farm would generate, if it were placed there.

This study doesn't come without its limitations, however, such as the fact that it doesn't consider the energy output of a specific tidal turbine, but rather a generic, bi-directional one, meaning it may not be entirely representative of the estuary's potential. Another limitation comes in the form of the simulation model itself, both in terms of its resolution (300x300 m) and also the output data time (one hour), as these aren't entirely representative of the estuary's resources. Another thing that was lacking was the consideration of multiple turbines in the simulation for a single cell. This stems from the fact that the way the Turbine Module was computed means that there can only be one turbine per cell.

Following the study carried out, some opportunities and suggestions for the making of future works are presented, in order to complement and develop upon the results obtained in this study.

With respect to the simulation model itself, it would benefit from having not only a higher grid cell resolution, but also from outputting data in more instances, in order to have a clearer picture of a site's hydrodynamics and energy potential. This can be easily solved through the use of a higher-resolution nested model in the simulation model used and by setting a lower output time so as to get more time instances from the simulation model. The assessment made would also benefit from determining the dynamics of multiple tidal turbines together, so as to see the influence they have on each other's energy production. Another interesting variation would be the use of a specific tidal turbine technology – hopefully one that has already been developed and is higher up on the readiness scale. That could add to the validation of a feasibility of the implementation of such a technology in settings beside urban environments, such as the Tagus estuary is to the city of Lisbon.

Finally, the Module Turbine that was coded into the MOHID software can be perfected into mimicking better a tidal turbine's reaction to a water current, namely taking into account the powertrain efficiency and considering a variating rotor power coefficient, based on the water current velocity. Such improvements would likely result in a more trustworthy result for a tidal turbine's electric energy output potential, on a specific assessment site.

REFERENCES

Antunes, C. (2013). *Caracterização do regime de marés* (p. 18). Faculdade de Ciências da Universidade de Lisboa (FCUL). https://sniambgeoviewer.apambiente.pt/Geodocs/geoportaldocs/Politicas/Agua/Ordenamento/SistemasMonitorizacaoLitoral/E_1.1.3.a_Regime_mares.pdf

ARH Tejo. (2011). *Plano de Gestão da Região Hidrográfica do Tejo* (p. 493). Ministério da Agricultura, Mar, Ambiente e Ordenamento do Território. https://www.apambiente.pt/_zdata/Politicas/Agua/ParticipacaoPublica/Documentos/ARHTejo/PGRH/2_PGRHTejo_versoextensa.pdf

Balsells Badia, Ó. (2017). *Implementation of the effect of turbines on water currents in MOHID Modelling System* [Instituto Superior Técnico]. https://upcommons.upc.edu/handle/2117/112828

Campuzano, F. J., Juliano, M., Sobrinho, J., dePablo, H., Brito, D., Fernandes, R., and Neves, R. (2017). Coupling Watersheds, Estuaries and Regional Oceanography through Numerical Modelling in the Western Iberia: Thermohaline Flux Variability at the Ocean-Estuary Interface. *Estuary*. https://doi.org/10.5772/intechopen.72162

Castro-Santos, L., Garcia, G. P., Estanqueiro, A., and Justino, P. A. P. S. (2015). The Levelized Cost of Energy (LCOE) of wave energy using GIS based analysis: The case study of Portugal.

International Journal of Electrical Power & Energy Systems, *65*, 21–25. https://doi.org/10.1016/j.ijepes.2014.09.022

Corsatea, T. D., and Magagna, D. (2014). *Overview of European Innovation Activities in Marine Energy Technology* (p. 60). Joint Research Centre - Institute for Energy and Transport. http://publications.jrc.ec.europa.eu/repository/bitstream/JRC90901/jrc-14-marinereport-online-dm.pdf

Det Norske Veritas. (2014). *Design of Offshore Wind Turbine Structures* (p. 238). DNV. https://rules.dnvgl.com/docs/pdf/DNV/codes/docs/2014-05/Os-J101.pdf

FCUL. (n.d.). *Previsão de Marés dos Portos Principais de Portugal*. Retrieved 5 September 2018, from http://webpages.fc.ul.pt/~cmantunes/hidrografia/hidro_mares.html

Hammons, T. J. (2011). Tidal Power in the UK and Worldwide to Reduce Greenhouse Gas Emissions. *International Journal of Engineering Business Management*, *3*(2), 16–28.

ICNF. (n.d.). *Geologia | Hidrologia | Clima* [Página]. Geologia, hidrologia e clima da Reserva Natural do Estuário do Tejo. Retrieved 19 September 2018, from http://www2.icnf.pt/portal/ap/r-nat/rnet/geo

IEA. (2016). *World Energy Outlook 2016*. International Energy Agency. https://www.iea.org/reports/world-energy-outlook-2016

Instituto Hidrográfico. (n.d.). *Tabela de Marés*. Tabela de Marés. Retrieved 27 December 2018, from http://www.hidrografico.pt/tabelamares

Kempener, R., and Neumann, F. (2014). *Tidal Energy - Technology Brief* (p. 36). International Renewable Energy Agency (IRENA). http://www.irena.org/DocumentDownloads/Publications/Tidal_Energy_V4_WEB.pdf

Legrand, C. (2009). *Assessment of Tidal Energy Resource - Marine Renewable Energy Guides* (p. 60). European Marine Energy Centre Ltd (EMEC). http://www.emec.org.uk/assessment-of-tidal-energy-resource/

Lewis, A., Estefen, S., Huckerby, J., Musical, W., Pontes, T., and Torres-Martinez, J. (2011). *Ocean Energy. In IPCC Special Report on Renewable Energy Sources and Climate Change Mitigation*. Cambridge University Press. http://www.ipcc-wg3.de/report/IPCC_SRREN_Ch06.pdf

Macedo, M. E. (2006). *Caracterização de Caudais do Rio Tejo* (p. 30). Ministério do Ambiente, do Ordenamento do Território e do Desenvolvimento Regional. http://www.ccdr-lvt.pt/files/fab372a0a4525eddaf1c20e1ab852a25.pdf

Manwell, J. F., McGowan, J. G., and Rogers, A. L. (2009). *Wind Energy Explained - Theory, Design and Application* (p. 705). http://ee.tlu.edu.vn/Portals/0/2018/NLG/Sach_Tieng_Anh.pdf

MARETEC. (n.d.). *MOHID Description: Description of the 3D water modelling system* (p. 112). MARETEC. http://www.mohid.com/PublicData/Products/Manuals/Mohid_Description.pdf

O Rourke, F., Boyle, F., and Reynolds, A. (2010). Tidal energy update 2009. *Applied Energy*, *87*(2), 398–409. https://doi.org/10.1016/j.apenergy.2009.08.014

Ocean Energy Systems. (2015). *International Levelised Cost Of Energy for Ocean Energy Technologies* (p. 48). International Energy Agency. https://www.ocean-energy-systems.org/news/international-lcoe-for-ocean-energy-technology/

Owen, A. (2008). Chapter 7 - Tidal Current Energy: Origins and Challenges. In T. M. Letcher (Ed.), *Future Energy* (pp. 111–128). Elsevier. https://doi.org/10.1016/B978-0-08-054808-1.00007-7

PORDATA. (n.d.-a). *Consumo de energia eléctrica: total e por tipo de consumo*. Retrieved 27 March 2019, from https://www.pordata.pt/Municipios/Consumo+de+energia+el%c3%a9ctrica+total+e+por+tipo+de+consumo-25-123

PORDATA. (n.d.-b). *Preços da electricidade para utilizadores domésticos e industriais (Euro/ECU)*. Retrieved 14 March 2020, from https://www.pordata.pt/Europa/Pre%C3%A7os+da+electricidade+para+utilizadores+dom%C3%A9sticos+e+industriais+(Euro+ECU)-1477

Portela, L. (1996). *Modelação matemática de processos hidrodinâmicos e da qualidade da água no estuário do Tejo* [Instituto Superior Técnico]. http://repositorio.lnec.pt:8080/xmlui/handle/123456789/8737

Prandle, D. (1984). Simple theory for designing tidal power schemes. *Advances in Water Resources*, *7*(1), 21–27. https://doi.org/10.1016/0309-1708(84)90026-5

Segura, E., Morales, R., and Somolinos, J. A. (2017). Cost Assessment Methodology and Economic Viability of Tidal Energy Projects. *Energies*, *10*(11), 1806. https://doi.org/10.3390/en10111806

Smart, G., and Noonan, M. (2018). *Tidal Stream and Wave Energy Cost Reduction and Industrial Benefit* (p. 21). Offshore Renewable Energy Catapult. https://www.marineenergywales.co.uk/wp-content/uploads/2018/05/ORE-Catapult-Tidal-Stream-and-Wave-Energy-Cost-Reduction-and-Ind-Benefit-FINAL-v03.02.pdf

SNIRH. (n.d.). *SNIRH :: Sistema Nacional de Informação de Recursos Hídricos*. Retrieved 14 March 2020, from https://snirh.apambiente.pt/index.php?idMain=

U.S. Energy Information Administration. (2018). *Levelized Cost and Levelized Avoided Cost of New Generation Resources in the Annual Energy Outlook 2018* (p. 20). U.S. Energy Information Administration. https://www.eia.gov/outlooks/archive/aeo18/pdf/electricity_generation.pdf

U.S. Energy Information Administration (EIA). (n.d.). *Tidal power*. Retrieved 14 March 2020, from https://www.eia.gov/energyexplained/hydropower/tidal-power.php

World Energy Council. (2016). *World Energy Resources - Marine Energy* (p. 79). World Energy Council. http://large.stanford.edu/courses/2018/ph240/rogers2/docs/wec-2016.pdf